

THE THREE-DIMENSIONAL STRUCTURE OF THE WARM LOCAL INTERSTELLAR MEDIUM. I. METHODOLOGY¹

JEFFREY L. LINSKY, SETH REDFIELD, BRIAN E. WOOD, AND NIKOLAI PISKUNOV²

JILA, University of Colorado and NIST Campus Box 440, Boulder, CO 80309-0440

Received 1999 April 26; accepted 1999 September 1

ABSTRACT

In this first in a series of papers, we develop a methodology for constructing three-dimensional models of the local interstellar cloud (LIC) and adjacent warm clouds in the local interstellar medium (LISM). Our models are based on the column density of neutral hydrogen gas ($N_{\text{H I}}$) inferred primarily from measurements of the deuterium column density toward nearby stars obtained from the analysis of *Hubble Space Telescope* ultraviolet spectra. We also use values of $N_{\text{H I}}$ inferred from spectra of hot white dwarfs and B-type stars obtained by the *Extreme Ultraviolet Explorer* satellite. These very different methods give consistent results for the three white dwarf stars in common. We assume that along each line of sight all interstellar gas moving with a speed consistent with the LIC velocity vector has a constant density, $N_{\text{H I}} = 0.10 \text{ cm}^{-3}$, and extends from the heliosphere to an edge determined by the value of $N_{\text{H I}}$ moving at this speed. A number of stars have velocities and/or depletions that indicate absorption by other warm clouds in their lines of sight. On this basis α Cen A and B and probably also ϵ Ind lie inside the Galactic center (G) cloud, HZ 43 and 31 Com lie inside what we call the north Galactic pole cloud, and β Cet is located inside what we call the south Galactic pole cloud. We show the locations of these clouds in Galactic coordinates. The Sun is located very close to the edge of the LIC toward the Galactic center and the north Galactic pole. The absence of Mg II absorption at the LIC velocity toward α Cen indicates that the distance to the edge of the LIC in this direction is ≤ 0.05 pc and the Sun should leave the LIC and perhaps enter the G cloud in less than 3000 yr. Comparison of LIC and total values of $N_{\text{H I}}$ toward pairs of stars with separations between $0^\circ.9$ and 20° reveals a pattern of good agreement so long as both stars lie within 60 pc of the Sun. Thus the LIC and perhaps also other nearby warm clouds have shapes that are smooth on these angular scales. In our second paper we will therefore fit the shape of the LIC with a set of smooth basis functions (spherical harmonics).

Subject headings: circumstellar matter — dust, extinction — infrared: ISM: lines and bands — ISM: abundances — molecular processes

1. INTRODUCTION

The Galactic environment in which the solar system resides provides the confining pressure for the heliosphere and is a convenient laboratory for studying physical processes in the interstellar medium. Since 1962, many authors (e.g., Munch & Unsold 1962; Vidal-Madjar et al. 1978; McClintock et al. 1978; Vallerga et al. 1993; Welty, Morton, & Hobbes 1996) have inferred the physical properties and column densities of low-density interstellar gas by analyzing the narrow absorption components in the cores of the resonance lines of Ca II, Na I, Mg II, and other species observed toward bright stars. The *Copernicus* and *International Ultraviolet Explorer* (IUE) satellites and then the Goddard High Resolution Spectrograph (GHRS) and Space Telescope Imaging Spectrograph (STIS) instruments on the *Hubble Space Telescope* (HST) have provided a powerful stimulus to this topic as the ultraviolet resonance lines of abundant ions are opaque, and the neutral hydrogen Lyman lines are sensitive to column densities of neutral gas nearly 5 orders of magnitude smaller than the metal-line tracers. Savage & Sembach (1996) and Frisch (1995) have provided comprehensive reviews of this topic.

Crutcher (1982) first noted that the spectra of many nearby stars spread over most of the sky contain narrow interstellar absorption features with velocities equal to (within measurement errors) the projection of a single velocity vector. Lallement & Bertin (1992) and Lallement et al. (1995) then demonstrated that the solar system is located inside a cloud of warm gas moving coherently with this same velocity vector. A critical piece of evidence is that interstellar neutral helium atoms, which flow through the heliosphere unimpeded by interactions with the solar wind, have the same velocity vector as the local interstellar gas (Witte et al. 1993). This cloud, which Lallement and collaborators call the “local interstellar cloud” (LIC), but is also called the “local fluff” by Frisch (1995) and the “surrounding interstellar cloud” (SIC) by Gayley et al. (1997), extends for several parsecs in most directions. A second cloud in the Galactic center hemisphere, which extends to within 1 pc of the Sun, is called the Galactic (G) cloud by Lallement & Bertin (1992) or the “squall line” cloud by Frisch (1995). Interstellar Ca II and Na I absorption at the G cloud velocity is typically observed toward stars that lie within about 40° of the star α Oph ($l = 36^\circ$, $b = +23^\circ$). These and other nearby clouds of warm gas constitute the local interstellar medium (LISM).

Frisch (1995, 1996) proposed a model for the local region of space in which the solar system and the LISM lie within a low-density region located near the inside of the Orion-Cygnus spiral arm. The LISM is embedded within a large superbubble of hot ($T \approx 10^6$ K), very low density ($n \approx 0.005$

¹ Based on observations with the NASA/ESA Hubble Space Telescope, obtained at the Space Telescope Science Institute, which is operated by the Association of Universities for Research in Astronomy, Inc., under NASA contract NAS5-26555.

² Now at Uppsala Astronomical Observatory, Box 515, S-751 20 Uppsala, Sweden.

TABLE 1
HYDROGEN COLUMN DENSITIES AND DISTANCES TO THE EDGE OF THE LOCAL CLOUD OBTAINED FROM GHRS SPECTRA

ID (1)	STAR (2)	SPECTRA (3)	d (pc) (4)	l (deg) (5)	b (deg) (6)	N_{D_1} (Measured) (7)	$N_{H I}$ (Total) (8)	$\langle n_{H I} \rangle$ (cm^{-3}) (9)	WHICH CLOUD? (10)	d_{edge} (pc)		REFERENCE (13)
										Total (11)	LIC (12)	
α C	α Cen A,B	E	1.35	316	-01	6.2(12)	4.1(17)	0.099	G	≥ 1.34	≤ 0.05	1
SI	Sirius	M	2.63	227	-09	5.4(12)	3.6(17)	0.044	LIC, 1	1.2	0.58	2
ϵ E	ϵ Eri ^a	E	3.22	196	-48	1.1(13)	7.1(17)	0.071	LIC	2.3	2.3	3
61	61 Cyg A ^a	E	3.48	082	-06	1.0(13)	6.8(17)	0.063	LIC, 1	2.2	1.0	4
ϵ I	ϵ Ind ^a	E	3.63	336	-48	1.6(13)	1.1(18)	0.095	LIC/G	3.6	?	5
PR	Procyon	M	3.50	214	+13	1.8(13)	1.2(18)	0.110	LIC, 1	≥ 3.5	2.2	6
40	40 Eri A ^a	E	5.04	201	-38	1.1(13)	7.1(17)	0.046	LIC	2.3	2.3	4
β G	β Gem	E	10.3	192	+23	2.7(13)	1.8(18)	0.056	LIC, 1	5.7	3.4	3
CA	Capella ^a	E	12.9	163	+05	2.8(13)	1.9(18)	0.047	LIC	6.2	6.2	7
β C	β Cas	E	16.7	118	-03	2.3(13)	1.5(18)	0.030	LIC	5.0	5.0	3
α T	α Tri	E	19.7	139	-31	2.9(13)	1.9(18)	0.031	LIC, 1	6.0	4.0	3
λ A	λ And ^a	E	25.8	110	-15	4.8(13)	3.2(18)	0.040	?	10.4	?	5
99	HR 1099	E	29.0	185	-42	2.1(13)	1.4(18)	0.016	LIC, 2	4.5	2.7	8
CE	β Cet	M	29.4	111	-81	5.1(13)	3.4(18)	0.037	SGP, 1	11.0	?	8
43	HZ 43	E	32.0	054	+84	1.3(13)	8.7(17)	0.0088	NGP	2.8	≤ 0.3	9
σ G	σ Gem	E	37.5	191	+23	2.2(13)	1.5(18)	0.013	LIC, 1	4.7	3.0	3
G1	G191-B2B	S	68.8	156	+07	...	2.0(18)	0.010	LIC, 1	6.6	5.5	10
31	31 Com	M	94.2	115	+89	1.3(13)	8.7(17)	0.0030	NGP	2.8	≤ 0.1	8
10	REJ 1032+	S	132	158	+53	...	5.2(18)	0.013	≥ 2	16.9	?	11
ϵ C	ϵ CMa	M	132	240	-11	...	4(17):	0.001:	LIC, 5	1.3:	0.9:	12
BC	β CMa	M	153	226	-14	$> 2(13)$	$> 2(18)$	> 0.004	4	> 6	?	13

NOTE.— $a(b) = a \times 10^b$. For col. (3), E: high-resolution GHRS ($\lambda/\Delta\lambda = 90,000$) echelle spectra; M: moderate-resolution ($\lambda/\Delta\lambda = 20,000$) spectra using G160M or G140M gratings; S: STIS E140M echelle ($\lambda/\Delta\lambda \approx 46,000$). Numerals in col. (10) indicate number of additional clouds observed.

^a Hydrogen wall absorption discovered.

REFERENCES.—(1) Linsky & Wood 1996; (2) Bertin et al. 1995; (3) Dring et al. 1997; (4) Wood & Linsky 1998; (5) Wood et al. 1996; (6) Linsky et al. 1995; (7) Linsky et al. 1993; (8) Piskunov et al. 1997; (9) Landsman et al. 1996; (10) Sahu et al. 1999; (11) Holberg et al. 1999; (12) Gry et al. 1995; (13) Dupin & Gry 1998.

cm^{-3}) plasma created by supernovae and stellar winds from the young stars in the Scorpius–Centaurus OB association located about 150 pc away (cf. Cox & Reynolds 1987). This conclusion is based in part on the velocity of the interstellar gas (the LIC cloud) which, in the local standard of rest (defined by the motion of nearby stars), flows from Galactic coordinates $l = 331^\circ.9$, $b = +4^\circ.6$. For the G cloud the upwind direction is $l = 334^\circ.5$, $b = +11^\circ.8$. The center of the Sco-Cen association lies nearly in the same direction: $l = 320^\circ$, $b = +15^\circ$. Since the LIC appears to be significantly ionized with $f_{\text{H}} = n_p/(n_p + n_{\text{H I}}) = 0.45 \pm 0.25$ (cf. Wood & Linsky 1997), it was likely heated by an energetic event in the Sco-Cen association more than 10^6 yr ago (Lyu & Bruhweiler 1996; Frisch 1996), perhaps when the superbubble was originally formed about 4×10^6 yr ago. Subsequent energetic events, such as supernovae, could have energized shocks that have distorted the superbubble into a series of incomplete shells, leading to the complex set of individual cloud fragments with slightly different velocities that now constitute the LISM. In particular, the G cloud could be a shell of a later superbubble event that began $\approx 400,000$ yr ago and is now located within a few parsecs of the Sun in the Galactic center direction.

Several approaches have been used in attempting to understand the morphology of the LIC and the other clouds in the LISM. One approach is to infer the location (in the Galactic plane and perpendicular to it) of contours of constant hydrogen column density obtained either directly from H I data or indirectly from Ca II, Mg II, or Na I data (e.g., Frisch & York 1983; Paresce 1984; Frisch 1990;

G nova et al. 1990). A second method is to infer the rough location of individual clouds or absorbing structures either in two or three dimensions (York & Frisch 1984; Bruhweiler 1996; Lallement et al. 1995) from absorption features with similar velocities. A third method is to infer the location of edges of individual clouds along different lines of sight using information from a combination of metal-line and H I data (Frisch 1994, 1996). The uncertainties associated with the use of metal lines described above and the absence of three-dimensionality in many of these models makes it difficult to assess their accuracy.

The objective of this series of papers is to build a detailed three-dimensional model of the LIC and to model other warm clouds in the LISM by using *the most accurate neutral hydrogen column densities* toward nearby stars. Our models are based primarily on analyses of high-resolution ultraviolet spectra observed with the GHRS and STIS instruments on *HST*. As a secondary data source we use interstellar neutral hydrogen densities obtained from the comparison of models of hot white dwarfs with extreme ultraviolet spectra obtained with the *Extreme Ultraviolet Explorer (EUVE)* spacecraft. We do not initially use H I column densities inferred from observations of metal lines (e.g., Na I, Ca II, Mg II, and Fe II), because the $N_{\text{Ca II}}/(N_{\text{H I}} + N_{\text{H II}})$ and $N_{\text{Mg II}}/(N_{\text{H I}} + N_{\text{H II}})$ ratios are known to vary by factors of 5–10 for different sight lines through warm interstellar gas (Sembach & Savage 1996; Piskunov et al. 1997; Frisch 1996). These gas ratios vary spatially as a result of different degrees of ionization and depletion onto grains. The price we pay for using only the hydrogen data is a model based

on a limited number of lines of sight, but each line of sight has an accurate column density of the dominant species (neutral hydrogen). We will then return to the question of whether Ca II column densities can provide useful information for constructing models.

The analysis of excellent GHRs spectra of the resonance lines of Mg II, Fe II, H I, and D I toward Capella ($d = 12.9$ pc) by Linsky et al. (1993) showed that the LIC gas is warm ($T = 7000 \pm 900$ K) and the nonthermal motions are very subsonic ($\xi = 1.6 \pm 0.6$ km s⁻¹). Both quantities include estimates of systematic errors. Analysis of spectra for the Procyon (Linsky et al. 1995), Sirius A (Bertin et al. 1995), and other lines of sight (Piskunov et al. 1997; Dring et al. 1997) confirm this LIC temperature, although the Procyon line of sight has a lower turbulence, $\xi = 1.21 \pm 0.27$ km s⁻¹. On the other hand, analysis of the ultraviolet spectra of α Cen (Linsky & Wood 1996) showed that the G cloud is cooler ($T = 5400 \pm 500$ K) with $\xi = 1.20 \pm 0.25$ km s⁻¹. The turbulence or line-of-sight velocity shear could be even smaller than 1.2 km s⁻¹, but this quantity is difficult to measure with the 3.5 km s⁻¹ spectral resolution of the GHRs. Frisch (1996) has suggested that the nonthermal broadening could be due to subparsec-scale structures with different velocities and physical properties. Welty et al. (1996) estimated that only 10% of the interstellar velocity components are resolved for unsaturated lines at the 3.6 km s⁻¹ resolution of the GHRs.

The density and geometry of the LIC are more difficult to measure for many reasons. First, one does not know a priori the geometrical extent of the LIC along the line of sight to a star, so the measured hydrogen column density, $N_{\text{H I}} = 3.086 \times 10^{18} d(\text{pc}) \langle n_{\text{H I}} \rangle$ cm⁻², determines only the average neutral hydrogen density along the line of sight. A general decrease in $\langle n_{\text{H I}} \rangle$ with increasing stellar distance (see Table 1) implies that the LIC extends only over a short distance and is probably surrounded in many directions by hot, low-density interstellar gas containing very little neutral hydrogen (Wood, Alexander, & Linsky 1996). The detection of additional velocity components in the warm gas toward even very nearby stars such as Procyon (3.50 pc), Sirius A (2.63 pc), and Altair (5 pc) (cf. Linsky et al. 1995; Bertin et al. 1995; Ferlet, Lallement, & Vidal-Madjar 1986) confirms that the LIC has dimensions of only a few parsecs, at least in these directions, with additional discrete warm gas clouds outside of the LIC. Second, until very recently there were excellent GHRs spectra available for only a very few lines of sight through the LISM, but many more observations are now available. Third, it is difficult to infer accurate hydrogen column densities from the analysis of Ly α absorption when $N_{\text{H I}} \sim 10^{18}$ cm⁻², a typical value for nearby stars, since the hydrogen lines are heavily saturated with line center optical depths $\geq 10^5$ and the column density corresponds to the flat part of the curve of growth where large changes in $N_{\text{H I}}$ produce only small changes in the absorption line profile. Also, estimates of $N_{\text{H I}}$ from measured column densities of other atoms or ions depend on uncertain abundances, interstellar depletion on grains, and ionization equilibria. We therefore adopt a different approach.

2. WHY DEUTERIUM IS AN ACCURATE PROBE OF THE HYDROGEN INTERSTELLAR ABSORPTION

In this paper we follow the approach of Bertin et al. (1995), who adopted the deuterium column density ($N_{\text{D I}}$) as

the most accurate way to measure $N_{\text{H I}}$ in the LIC toward nearby stars. We will apply this technique to the available sample of GHRs spectra of stellar Ly α lines to infer the three-dimensional geometry of the LIC. We believe that the deuterium Ly α line usually provides the most accurate means of measuring $N_{\text{H I}}$ along short lines of sight for the following reasons:

1. Measurements of the D/H ratio along many lines of sight are consistent with a constant D/H ratio in the LIC. Since an accurate value for the primordial D/H ratio would provide a critical constraint on theories of the early universe, attempts have been made to measure D/H in many different astronomical environments. For the LISM, measuring the ratio of $N_{\text{D I}}/N_{\text{H I}}$ by analysis of the deuterium and hydrogen Ly α absorption superimposed upon the chromospheric Ly α emission line of a nearby star is a useful approach, since hydrogen and deuterium should have the same degree of ionization, association into molecules, and adsorption onto grains in the warm LISM gas. Linsky et al. (1993) derived $\text{D}/\text{H} = 1.65^{+0.07}_{-0.18} \times 10^{-5}$ from a careful analysis of the interstellar Ly α absorption toward Capella. Subsequent analysis of the interstellar absorption superimposed on Capella's Ly α emission lines at opposite orbital quadratures (Linsky et al. 1995) led to essentially the same result, $\text{D}/\text{H} = 1.60^{+0.14}_{-0.19} \times 10^{-5}$. A reanalysis of these data by Vidal-Madjar et al. (1998) using different analysis software gives $\text{D}/\text{H} = 1.56 \pm 0.1 \times 10^{-5}$, in excellent agreement with previous results. Analysis of interstellar Ly α absorption toward stars with small radial velocities and narrow emission lines, such as α Cen A and B (Linsky & Wood 1996), resulted in larger uncertainties in the D/H ratio. Wood et al. (1996) therefore developed a new technique to infer $N_{\text{H I}}$ from the Ly α wings of stars with high radial velocities. They found that $\text{D}/\text{H} = 1.6 \pm 0.4 \times 10^{-5}$ for the ϵ Ind (3.63 pc) line of sight, consistent with the Capella measurement. Subsequent analyses of GHRs spectra for several other lines of sight provide similar D/H ratios (Dring et al. 1997; Piskunov et al. 1997), but there is evidence for lower values of the D/H ratio beyond the LIC toward G191-B2B (cf. Lemoine et al. 1996; Vidal-Madjar et al. 1998) and toward δ Ori A (Jenkins et al. 1999). The results for the LIC are consistent with the mean value of $\text{D}/\text{H} = 1.8 \pm 0.4 \times 10^{-5}$ derived from *Copernicus* observations of the higher Lyman lines toward OB stars as distant as 1 kpc (York & Rogerson 1976), although some of these lines of sight show D/H ratios with considerably smaller values (cf. Ferlet, Lemoine, & Vidal-Madjar 1996).

In a recent review of the D/H measurements obtained from GHRs spectra, Linsky (1998) finds that the mean value of D/H in the LIC is $1.50 \pm 0.10 \times 10^{-5}$ and the mean value for 12 lines of sight in the LISM is $1.47 \pm 0.18 \times 10^{-5}$. All of the data points have 1 σ error bars that lie within the 1 σ uncertainty of the mean values. One might expect the LISM to be well mixed at least on distance scales of 10 pc, since for typical flow speeds of 10 km s⁻¹ the mixing timescale is 10⁶ yr. The LISM value for the D/H ratio is generally believed to be a lower limit to the primordial D/H ratio because deuterium is easily destroyed by nuclear reactions inside stars and the resulting deuterium-depleted gas is recycled into the interstellar medium by stellar winds and supernova explosions (e.g., Walker et al. 1991). Mullan & Linsky (1999), however, argue that stellar flares may eject a sufficient amount of deuterium into the ISM to invalidate this conclusion.

2. Deuterium column densities usually can be measured much more accurately than hydrogen column densities. For nearby stars, typical line center optical depths for the deuterium Ly α line are about unity, whereas central optical depths for the hydrogen line are 10^5 – 10^6 . Thus the amount of absorption in the deuterium line directly yields an accurate value for N_{D_1} that is nearly independent of the optical depth of the hydrogen Ly α line and of the location of absorbers in one or many discrete clouds moving at different velocities. For the heavily saturated interstellar hydrogen line, however, the optical depth depends on the uncertain shape of the intrinsic stellar emission line, on the line-broadening parameter, and on the possible presence of small amounts of hot, neutral gas with significant velocity shifts (Linsky & Wood 1996; Wood & Linsky 1998). For A-type stars like Sirius A, the shape of the photospheric Ly α absorption cannot be disentangled unambiguously from the interstellar hydrogen absorption, and N_{H_1} can be estimated most accurately from the measured N_{D_1} and the assumed D/H ratio (cf. Bertin et al. 1995).

For $\log N_{H_1} < 18.0$ the amount of hydrogen absorption at the center of the deuterium line (displaced -81 km s^{-1} relative to hydrogen) is sufficiently small that the “continuum” at the location of the deuterium absorption can be reconstructed by simple interpolation and the value of N_{D_1} can be derived independent of N_{H_1} (Linsky & Wood 1996). For larger values of N_{H_1} up to about $\log N_{H_1} = 18.7$, it is possible to model the wing of the hydrogen absorption at the position of the deuterium line (Linsky et al. 1993), so that one can still infer the “continuum” and thus derive N_{D_1} accurately. For larger values of N_{H_1} the analysis becomes uncertain.

3. For the α Cen line of sight, the center of the hydrogen absorption is redshifted by 2.2 km s^{-1} relative to the D I, Fe II, and Mg II interstellar lines. This was interpreted by Linsky & Wood (1996) and by Gayley et al. (1997) as due to absorption by decelerated hot hydrogen located near the heliopause, the so-called hydrogen wall. Subsequently, hydrogen wall absorption was discovered around the stars ϵ Ind, λ And, ϵ Eri, 61 Cyg A, 40 Eri A, and Capella (Wood et al. 1996; Wood & Linsky 1998; Dring et al. 1997; Vidal-Madjar et al. 1998) on the basis of velocity shifts of the hydrogen absorption relative to other interstellar lines. These stars are noted in Table 1 to show how common this phenomenon could be. GHRs observations of interplanetary hydrogen (e.g., Clarke et al. 1998) confirm that the hydrogen gas inflowing from the LISM is heated and decelerated. Ignoring these extra blueshifted or redshifted absorption features, we find factor of 2 uncertainties in N_{H_1} , but the much less opaque deuterium line is unaffected because the deuterium opacity in the hydrogen wall is minuscule. Thus the deuterium absorption leads to an accurate measurement of interstellar N_{H_1} , independent of the presence of hydrogen walls around the Sun or the star.

3. DISTANCE TO THE EDGE OF THE LIC ALONG DIFFERENT LINES OF SIGHT

3.1. Hydrogen Column Densities in the LIC

We list in Table 1 the 15 cool stars, one A-type star (Sirius A), and two hot white dwarfs (G191-B2B and HZ 43) for which accurate deuterium or hydrogen column densities have been measured from GHRs or STIS spectra. Also included are two B-type stars (ϵ CMa and β CMa) for which

rough H or D column densities have been measured with the GHRs, and one hot white dwarf (REJ 1032+535) for which an H column density has been measured with the STIS instrument on *HST*. High-resolution GHRs ($\lambda/\Delta\lambda = 90,000$) echelle spectra were analyzed for the interstellar absorption toward 14 of these stars (designated by an “E” in col. [3]), while moderate-resolution ($\lambda/\Delta\lambda = 20,000$) spectra were obtained using the G160M or G140M gratings and analyzed for six stars (designated by an “M” in col. [3]). The moderate-resolution spectra do not fully resolve the deuterium lines, but they have sufficient resolution to infer accurate equivalent widths and column densities for these lines, which have optical depths close to unity. Table 1 also lists one hot white dwarf, REJ 1032+535, recently studied with the STIS E140M echelle (designated by an “S” in col. [3]), which has a resolution of $\lambda/\Delta\lambda \approx 46,000$. Columns (4)–(6) in Table 1 list the Hipparcos Catalogue distances (Perryman et al. 1997) and Galactic coordinates. Figure 1 shows the location in Galactic coordinates of the GHRs targets (marked by their two-symbol identifiers listed in col. [1] of Table 1). For each star except G191-B2B, REJ 1032+535, and ϵ CMa, we list in column (8) the hydrogen column density obtained from the relation $N_{H_1} = N_{D_1}/1.5 \times 10^{-5}$, rather than using the value of N_{H_1} published in the original paper. In most cases the published and our inferred values of N_{H_1} are in very close agreement, but for α Cen and Sirius, for example, the published values of N_{H_1} have large uncertainties, and for all of the stars the inferred value of N_{H_1} should be more accurate than the directly measured value for the reasons given in the previous section.

In their analysis of GHRs spectra of G191-B2B, Vidal-Madjar et al. (1998) concluded that the average D/H ratio through the three clouds in the line is $1.12 \pm 0.08 \times 10^{-5}$, although they concluded that the data are consistent with $D/H = 1.5 \times 10^{-5}$ in the LIC. We infer $N_{H_1}(\text{LIC}) = 7.3 \times 10^{17} \text{ cm}^{-2}$ from their measured value of $N_{D_1}(\text{LIC}) = 1.1 \times 10^{13} \text{ cm}^{-2}$ and the assumption that $(D/H)_{\text{LIC}} = 1.5 \times 10^{-5}$. Very recently Sahu et al. (1999) have analyzed new STIS observations of G191-B2B and reanalyzed the previous GHRs spectra. They conclude that there is only one velocity component in addition to the LIC component and that the D/H ratios in both components are consistent with $D/H = 1.5 \times 10^{-5}$. They also present a very plausible explanation for why their conclusions differ from those presented by Vidal-Madjar et al. (1998). Sahu et al. argue that the scattered light, which is especially important in the Ly α region, is much better characterized for the STIS instrument than for the GHRs. We therefore adopt the Sahu et al. values of $N_{H_1} = 2.04 \times 10^{18} \text{ cm}^{-2}$ for the total hydrogen column density and $N_{H_1}(\text{LIC}) = 1.72 \times 10^{18} \text{ cm}^{-2}$.

Interstellar absorption is ascribed to the LIC or the G cloud depending on whether the observed heliospheric velocity of the main absorption component lies within about 1 km s^{-1} of the projected velocity of the LIC or G cloud vector (Lallement & Bertin 1992). For ϵ Ind the projections of the two cloud vectors are nearly the same, and we cannot determine on the basis of the measured velocities alone whether the line of sight passes through one or both clouds. For the two stars located near the north Galactic pole (31 Com and HZ 43), the measured velocities are inconsistent with *both* the LIC and G clouds, and we list in column (10) “NGP” to indicate that a different cloud (which we tentatively call the “north Galactic pole cloud”) is observed. For 11 stars one or more additional clouds are

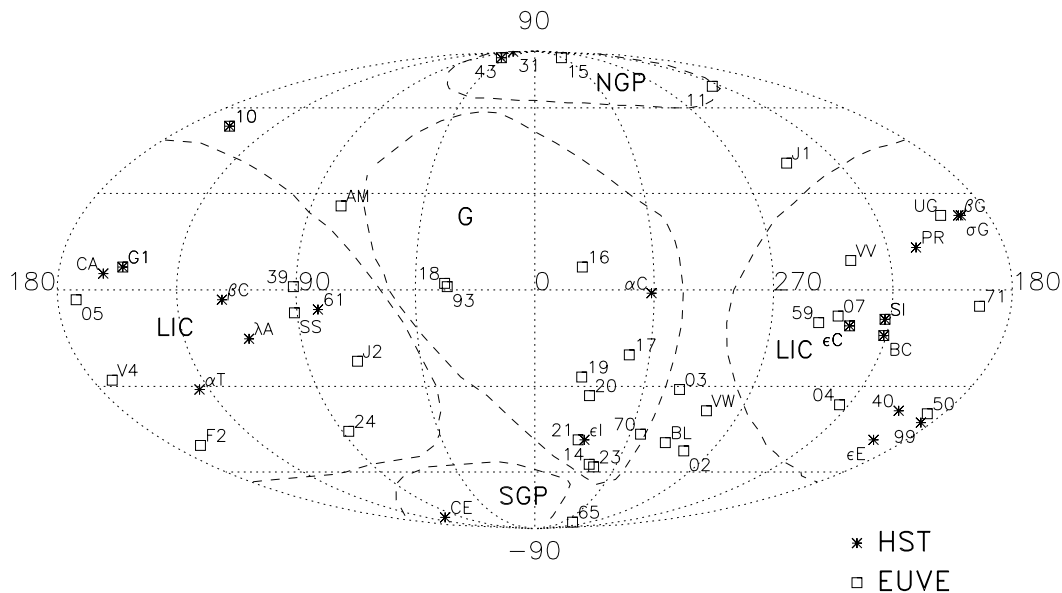


FIG. 1.—Locations of the *HST* and *EUVE* target stars in Galactic coordinates. Galactic north is at the top, $l = 0^\circ$ is the central meridian, and Galactic longitude increases toward the left with the $l = 180^\circ$ meridian on the far left and far right. Asterisk symbols show the *HST* targets and square symbols show the *EUVE* targets. The two-symbol identifiers for each star are listed in col. (1) of Tables 1 and 2. Dashed lines show the approximate edges of significant absorption by the local interstellar cloud (LIC), G cloud (G), north Galactic pole cloud (NGP), and south Galactic pole cloud (SGP).

observed. The value of $N_{\text{H I}}$ listed for ϵ CMa (Gry et al. 1995) is uncertain, because there are six clouds in the line of sight, no direct measurement of $N_{\text{D I}}$, and only an indirect inference of $N_{\text{H I}}$ from $N_{\text{N I}}$. The value of $N_{\text{H I}} > 1.7 \times 10^{18} \text{ cm}^{-2}$ for the β CMa line of sight that was estimated from $N_{\text{D I}}$ (Dupin & Gry 1998) is very similar to $N_{\text{H I}} = 1.6 \times 10^{18} \text{ cm}^{-2}$ inferred from *Copernicus* observations of the Ly β line (Gry et al. 1995) and the *EUVE* derived value of $N_{\text{H I}} = 2.0 \times 10^{18} \text{ cm}^{-2}$ (see Table 2). One of the interstellar absorption components toward β Cet (located near the south Galactic pole) is consistent with the projected LIC velocity, but we believe that most of the gas in this line of sight is in a different cloud, which we call the south Galactic pole (SGP) cloud, because the Mg π /H γ ratio is anomalously high (Piskunov et al. 1997) compared with all studied lines of sight through the LIC. For seven stars no absorption is seen at the predicted velocity of the LIC. For three of these stars (α Cen, HZ 43, and 31 Com), we could estimate upper limits to the hydrogen column density through the LIC, but for four stars (λ And, β Cet, REJ 1032+535, and β CMa) we could not estimate hydrogen column densities through the LIC. These values are small and are designated in column (12) by a “?” symbol.

3.2. Path Lengths along Lines of Sight through the LIC

To determine the distance from the Sun to the edge of the LIC or G cloud along a line of sight, one must either know that the star is located inside the cloud or assume a unique value for $n_{\text{H I}}$ inside the cloud. For the G cloud we assume that $n_{\text{H I}} = 0.10 \text{ cm}^{-3}$ because both α Cen and ϵ Ind (which could be seen through the G cloud given its absorption-line velocity) show the same density, the 1.35 pc distance to α Cen is extremely short, and there is no evidence for a second interstellar velocity component along the α Cen line of sight. Thus, the more distant edge of the G cloud (or LIC) lies beyond α Cen and ϵ Ind. The absence of absorption at the projected velocity of the LIC toward α Cen means that

the Sun lies very close to the boundary between the LIC and the G cloud, as noted by Lallement et al. (1995). We discuss this further in Linsky & Redfield (1999).

The largest mean density for a line of sight through the LIC is $\langle n_{\text{H I}} \rangle = 0.11 \text{ cm}^{-3}$ for the Procyon line of sight. However, there are two velocity components in the Procyon line of sight. The main component, with 64% of the total column density (as seen in the Mg π lines), lies at the projected LIC velocity; the second component has a velocity 2.6 km s^{-1} larger, indicating a separate cloud that likely lies outside of the LIC. In the absence of additional information, we will assume that the two clouds fill the sight line and have the same density. In this case the LIC extends 64% of the way to Procyon, and we assume the same value of $N_{\text{H I}}$ in the LIC and the other cloud. With these assumptions, the LIC appears to have essentially the same neutral hydrogen density as the G cloud.

Column (11) in Table 1 lists the distance to the edge of the warm LISM gas obtained by assuming that the mean density of the gas along the line of sight is $n_{\text{H I}} = 0.10 \text{ cm}^{-3}$ and the gas extends from the heliosphere uniformly until $d_{\text{edge}}(\text{total}) = N_{\text{H I}}/3.086 \times 10^{17} \text{ pc}$. Column (12) of Table 1 lists the distance to the edge of the LIC, $d_{\text{edge}}(\text{LIC})$, computed either from the D I column density for the LIC component or from $d_{\text{edge}}(\text{total})$ multiplied by the fraction of the total Mg π column density at the LIC velocity. Column (13) of Table 1 lists the references for the data. When two or more components are visible in Mg π , we assume that the relative amount of H I in the components is the same as for Mg π . This is obviously an approximation as the depletion and ionization of magnesium likely differ among the clouds. For α Cen the distance to the edge of the LIC is $\leq 0.05 \text{ pc}$ since no Mg π absorption is seen at the LIC velocity. For Sirius A, about half of the gas is moving at the LIC velocity, so $d_{\text{edge}}(\text{LIC}) = 0.58 \text{ pc}$. For Procyon, 64% of the gas is at the LIC velocity, so $d_{\text{edge}}(\text{LIC}) = 2.2 \text{ pc}$. For ϵ Ind, the projected LIC and G cloud velocities are the same, and there-

TABLE 2
LISM PARAMETERS OBTAINED FROM EUVE SPECTRA

ID (1)	Star (2)	d (pc) (3)	l (deg) (4)	b (deg) (5)	$N_{\text{H I}}$ (total) (6)	$\langle n_{\text{H I}} \rangle$ (cm^{-3}) (7)	Which Cloud? (8)	d_{edge} (pc) (Total) (9)	Reference (10)
SB	Sirius B	2.63	227	-09	5.2(17)	0.064	LIC, 1	1.7	1
16	REJ 1623-392	12.8	342	+07	3.2(18)	0.081	G ^a	10.3	2, 3
43	HZ 43	32.0	054	+84	8.7(17)	0.0088	NGP	2.8	4
					8.3(17)	0.0084		2.7	5
					9.3(17)	0.0094		3.0	6
50	GD 50	37	187	-39	8.7(17)	0.0076	LIC	2.8	6
14	HD 149499B	37.0	330	-57	7(18)	0.061	G ^a	23	3, 8
71	GD 71	42	192	-05	6.3(17)	0.0048	LIC	2.0	4
		51			8.4(17)	0.0053		2.7	5
93	BPM 93487	42	033	+01	2.9(18)	0.022	G?	9.4	5
18	REJ 1847+019	44	034	+02	2.2(18)	0.016	G?	7.1	9
J2	J2126+193	46	070	-22	2.5(18)	0.018	?	8.1	10
V4	V471 Tau B	46.8	172	-28	1.5(18)	0.010	LIC	4.8	11
39	GD 394	50	091	+01	4.4(18)	0.028	?	14.2	12
65	GD 659	58	299	-84	2.6(18)	0.014	SGP?	8.4	13
		57			2.9(18)	0.016		9.4	5
20	REJ 2009-605	62	337	-33	2.1(19)	0.11	G?	68	5
VW	VW Hyi	65?	285	-38	~6(17)	0.003	?	1.9	14
G1	G191-B2B	68.8	156	+07	2.1(18)	0.010	LIC, 1	6.8	4, 15
15	GD 153	69	317	+84	9.8(17)	0.0046	?	3.2	3, 4
		72			7.8(17)	0.0035		2.5	5
24	GD 246	72	087	-45	1.3(19)	0.058	?	42	5, 16
F2	Feige 24	74.4	166	-50	3.0(18)	0.013	?	9.7	4
SS	SS Cyg	75?	091	-07	~6(19)	0.26	?	-	17
AM	AM Her	75?	078	+26	7.4(19)	0.32	?	-	18
17	REJ 1746-706	76	323	-20	1.8(19)	0.077	G?	58	19
04	MCT 0455	90	229	-36	1.3(18)	0.0047	?	4.2	4
UG	U Gem	90	199	+23	3.2(19)	0.11	?	90	14
19	J1925-565B	110?	341	-27	3.7(19)	0.11	G?	110	10
05	J0515+326	120?	173	-03	8.9(18)	0.024	LIC?	29	10
J1	J1016-053	127	248	+40	2.7(19)	0.069	?	87	20
21	REJ 2156-546	129	339	-48	5.9(18)	0.015	G?	19.0	5
εC	ε CMa	132	240	-11	9(17)	0.0024:	LIC, 5	2.9	21
BL	BL Hyi	132	296	-49	~3(19)	0.074	?	97	22
10	REJ 1032+535	135	158	+53	4.0(18)	0.0096	?	12.9	5
		132			4.2(18)	0.0103	≥2	13.6	23
07	REJ 0720-318	136	245	-08	2.3(18)	0.0055	?	7.4	24
03	REJ 0317-853	136	300	-31	2.7(19)	0.064	?	87	25
11	PG 1123+189	139	232	+69	1.0(19)	0.023	NGP?	32	5
VV	VV Pup	145	240	+09	2.8(19)	0.063	?	91	26
BC	β CMa	153	226	-14	2(18):	0.0042:	4	6.5:	27
59	HD 59635B	171	252	-10	2(19)	0.038	LIC?	65	28
23	REJ 2324-547	185	327	-58	4.0(18)	0.0070	G?	12.9	5
02	J0228-613	199	284	-52	2.1(19)	0.034	?	68	10
70	J2353-703	?	310	-46	1.1(19)	?	G?	36	10

NOTE.— $a(b) = a \times 10^b$. Numerals in col. (8) indicate number of additional clouds observed.

^a Assigned to the G cloud on the basis of *IUE* radial velocities (Holberg et al. 1998b).

REFERENCES.—(1) Holberg et al. 1998a; (2) Dupuis & Vennes 1996; (3) Holberg et al. 1998b; (4) Dupuis et al. 1995; (5) Barstow et al. 1997; (6) Barstow et al. 1995a; (7) Vennes et al. 1996a; (8) Napiwotzki et al. 1996; (9) Craig et al. 1997; (10) Vennes et al. 1998; (11) Cully et al. 1996; (12) Barstow et al. 1996; (13) Holberg et al. 1995; (14) Long et al. 1996; (15) Lanz et al. 1996; (16) Vennes et al. 1993; (17) Mauche, Raymond, & Mattei 1995; (18) Paerels et al. 1996; (19) Dupuis & Vennes 1997; (20) Vennes et al. 1997b; (21) Cassinelli et al. 1995; (22) Szkody et al. 1997; (23) Holberg et al. 1999; (24) Burleigh, Barstow, & Dobbie 1997; (25) Barstow et al. 1995b; (26) Vennes et al. 1995; (27) Cassinelli et al. 1996; (28) Vennes et al. 1998.

fore the measured total hydrogen column density does not provide an unambiguous value for the distance to the edge of the LIC in this direction. Capella shows only one velocity component, indicating that $d_{\text{edge}}(\text{LIC}) = 6.2$ pc along this line of sight, but the large value of ξ suggests that another cloud with nearly the same velocity could be present. If our assumption that the warm gas toward Procyon completely fills the line of sight is incorrect, then $N_{\text{H I}}$ will be somewhat larger than 0.10 cm^{-3} and the distances to the edge of the

LIC will shrink by the same factor. In particular, a recent analysis of the diffuse backscattered $\text{Ly}\alpha$ radiation observed by the *Voyager 1* and *Voyager 2* spacecraft (Quémerais et al. 1995) suggests that $N_{\text{H I}} = 0.16 \text{ cm}^{-3}$ just outside of the heliosphere. However, Scherer et al. (1999) conclude that even with the best available high-resolution GHRS spectra of the interplanetary diffuse backscattered $\text{Ly}\alpha$ emission, it is not possible to determine a unique set of LISM parameters including a value for $N_{\text{H I}}$. Thus we believe that $N_{\text{H I}} =$

0.10 cm^{-3} determined from the LISM H I column densities is the best available value for the parameter.

3.3. Path Lengths from EUVE Spectral Data

Analysis of *EUVE* spectra of hot white dwarfs, B-type stars, and cataclysmic binaries observed through the hydrogen Lyman continuum provides an independent method for determining the interstellar $N_{\text{H I}}$ values but without velocity information. In their study of six white dwarfs, Dupuis et al. (1995) fitted the spectra of three stars with pure-hydrogen model atmospheres and the other three stars with model atmospheres containing metals. They estimated that their values of $N_{\text{H I}}$ listed in Table 2 are uncertain by $\leq 10\%$. We list in Table 2 the published measurements of $N_{\text{H I}}$ along the lines of sight to 31 white dwarfs, two B-type stars, and six cataclysmic binaries located within 200 pc of the Sun that have been obtained from analyses of *EUVE* spectra. The locations of these targets in Galactic coordinates are shown in Figure 1 using the two-symbol identifiers in column (1) of Table 2. For five stars (Sirius B, HZ 43, G191-B2B, ϵ CMA, and β CMA) we list the intervening interstellar clouds inferred from GHRs spectra of these lines of sight. In the second paper we show that the absorption toward GD 50, GD 71, and V471 Tau is primarily through the LIC (Redfield & Linsky 2000). *IUE* spectra of REJ 1623–392, HD 149499B, and GD 153 (Holberg et al. 1998b) show absorption at the predicted velocity of the G cloud. For the remaining stars the identity of the absorbing cloud is guessed from the Galactic coordinates of the star (col. [8] in Table 2 shows the cloud name followed by a “?”) or is listed as unknown (indicated by “?”). High-resolution spectra are needed for those stars to determine what fractions of the total hydrogen column densities are in the LIC and what fractions are in other clouds along the lines of sight. Since many of the relatively distant stars have low hydrogen column densities, the filling fractions along these lines of sight are small and the distances to the edge of the warm LISM gas are similar to the distances derived from the late-type stars. While a number of authors (e.g., Dupuis et al. 1995; Vennes et al. 1993; Vallerga & Welsh 1995) have argued that the hydrogen along these lines of sight is predominately neutral, there are measurements showing that the hydrogen may be about half-ionized (e.g., Wood & Linsky 1997; Holberg et al. 1999).

The Ly α line and a number of metal lines in the spectrum of the white dwarf G191-B2B were observed with the GHRs (Lemoine et al. 1996; Vidal-Madjar et al. 1998) and STIS (Sahu et al. 1999). Two velocity components were detected along this line of sight, with the component at the expected LIC velocity containing most of the absorption. The total value of $N_{\text{H I}} = 2.04 \times 10^{18} \text{ cm}^{-2}$ derived by Sahu et al. (1999) is consistent with the *EUVE* value ($N_{\text{H I}} = 2.1 \times 10^{18} \text{ cm}^{-2}$). The value of $N_{\text{H I}} = 8.7 \times 10^{17} \text{ cm}^{-2}$ inferred from the GHRs deuterium line data for the hot white dwarf HZ 43 is very similar to the value of $N_{\text{H I}} = (8.3\text{--}9.3) \times 10^{17} \text{ cm}^{-2}$ obtained from three different analyses of its *EUVE* spectrum. The estimate of $N_{\text{H I}} = 5.2^{+1.4}_{-1.0} \times 10^{17} \text{ cm}^{-2}$ toward the white dwarf Sirius B based on *EUVE* and *IUE* spectra (Holberg et al. 1998b) is similar to the GHRs value of $N_{\text{H I}} = 3.6 \times 10^{17} \text{ cm}^{-2}$ toward Sirius A. Also, for REJ 1032+535 the measured value of $N_{\text{H I}} = 5.2 \times 10^{18} \text{ cm}^{-2}$ obtained from a STIS ultraviolet spectrum is similar to the values $N_{\text{H I}} = (4.0\text{--}4.2) \times 10^{18} \text{ cm}^{-2}$ obtained from *EUVE* spectra. Since analyses of the ultraviolet and *EUVE* spectra of hot white dwarfs are providing consistent values of $N_{\text{H I}}$, we will construct in a follow-up paper a model of the LIC based on both data sets (Redfield & Linsky 2000).

There are also estimates of the hydrogen column densities along lines of sight toward a larger number of white dwarfs obtained by comparing the EUV emission computed from white dwarf model atmospheres with EUV broadband *photometry* acquired by the Wide Field Camera (WFC) on *ROSAT* or by *EUVE* (e.g., Vennes et al. 1996b). Table 3 compares the values of $N_{\text{H I}}$ derived by Marsh et al. (1997) from the analysis of WFC photometry with hydrogen columns derived from *EUVE* and/or GHRs spectra. Of the 16 stars in this sample, only two (REJ 1126+18 and REJ 2009–60) show good agreement between the photometric and spectroscopic values. This consistent pattern of disagreement shows that the photometric values cannot now be used for estimating the geometry of the LISM. The large uncertainty in the photometric values presumably is due to the need for extremely precise atmospheric models because the photometry contains very little information.

We also include in Table 2 estimates of $N_{\text{H I}}$ toward the B-type stars ϵ CMA (Cassinelli et al. 1995) and β CMA (Cassinelli et al. 1996) obtained by comparing *EUVE*

TABLE 3
COMPARISON OF HYDROGEN COLUMN DENSITIES ($N_{\text{H I}}/10^{18}$) TOWARD WHITE DWARFS BY DIFFERENT TECHNIQUES

Star	Name	WFC Photometry	<i>EUVE</i> Spectroscopy	<i>HST</i> Spectroscopy
REJ 0029–63		$25.3^{+4.6}_{-4.1}$	200	...
REJ 0053–32	GD 659	$5.4^{+1.6}_{-1.3}$	2.6, 2.87	...
REJ 0235+03	Feige 24	$0.9^{+0.7}_{-0.2}$	3.0	...
REJ 0348–00	GD 50	$22.6^{+5.7}_{-5.1}$	0.87	...
REJ 0350+17	V471 Tau	$8.5^{+3.2}_{-2.2}$	1.5	...
REJ 0505+52	G191-B2B	...	2.1	2.0
REJ 0552+15	GD 71	$2.3^{+1.5}_{-1.2}$	0.63, 0.84	...
REJ 0645–16	Sirius A, B	$11.9^{+2.1}_{-1.9}$...	0.36
REJ 0715–704		$26.1^{+3.3}_{-3.2}$	210	...
REJ 1126+18	PG 1123+189	$9.6^{+2.3}_{-3.2}$	10.2	...
REJ 1316+29	HZ 43	$5.2^{+1.6}_{-1.7}$	0.87, 0.83, 0.93	0.87
REJ 1623–39		$1.8^{+1.9}_{-1.6}$	3.2	...
REJ 1746–706		$13.2^{+16.0}_{-7.5}$	18	...
REJ 2009–60		$21.0^{+3.2}_{-3.2}$	20.9	...
REJ 2156–54		$13.8^{+3.1}_{-2.8}$	5.87	...
REJ 2312+10	GD 246	$18.7^{+2.0}_{-4.1}$	13.1	...

spectra with theoretical models. The factor of 2 discrepancy between the hydrogen column toward ϵ CMA obtained from the GHRS and *EUVE* spectra is probably due more to the confusion of six clouds along the line of sight than to the difficulty in modeling the EUV spectra of B-type stars. On the other hand, the estimate of $N_{\text{H I}}$ for the line of sight to β CMA based on *EUVE* spectra is consistent with the values obtained from *Copernicus* (Gry, York, & Vidal-Madjar 1985) and GHRS spectra (Dupin & Gry 1998). The very large number of assumptions that are needed to analyze coronal spectra of cool stars makes any estimate of $N_{\text{H I}}$ from *EUVE* spectra of cool stars uncertain at this time.

4. ASTRONEPHOGRAPHY: THE SURFACE OF THE LIC

Tables 1 and 2 list estimated distances or upper limits to the edge of the LIC for 19 lines of sight and to the edge of the total amount of warm gas in the LISM for 54 lines of sight (six stars are listed in both tables). Figure 1 shows the rough outlines of the clouds in Galactic coordinates based on the lines of sight for which we have enough velocity information to make a sensible decision. For both calculations the density of neutral hydrogen is assumed to be $n_{\text{H I}} = 0.10 \text{ cm}^{-3}$ and the warm gas is assumed to extend continuously from the outer heliosphere to a distance corresponding to the hydrogen column density. Beyond that distance the interstellar medium is assumed to be hot with insignificant neutral hydrogen column density. We must make these simplifying assumptions, because there is no certain way to determine the location of the absorbing gas along a line of sight. This model has the virtue of simplicity, but it is not unique.

The study of interstellar cloud morphology is a relatively new research topic that deserves a new name. In analogy with “geography,” we propose the name “astronephography” based on the Greek word $\nu\epsilon\phi\omicron\sigma$ (*nephos*), meaning “cloud.”

4.1. The Maximum Angular Scale for Similar LISM Properties

The first question to ask concerning the LIC is whether its shape is relatively smooth or irregular over angular scales of $\sim 10^\circ$. To answer this question we compare in Table 4 the neutral hydrogen column densities of gas moving with the LIC velocity vector, $N_{\text{H I}}(\text{LIC})$, and of the total amount of warm LISM gas independent of velocity, $N_{\text{H I}}(\text{total})$, for pairs of nearby stars listed in Tables 1 and 2 in order of increasing angular separation from 0.9° to 20° . We describe the agreement in column density by the ratio of the largest to the smallest value: category A (ratio < 1.25), category B (ratio < 1.5), category C (ratio < 2.0), and category D (ratio > 2.0). Table 4 contains a comparison of LIC column densities for six star pairs in Table 4. Five of the six are category A, indicating excellent agreement for stars up to about 13° apart. One disagreement is the Sirius/ ϵ CMA pair, which may be explained by ϵ CMA (and β CMA) being viewed through an interstellar tunnel of hot gas (Welsh 1991), whereas Sirius lies outside the tunnel. The excellent agreement of five out of six LIC star pairs is evidence that the LIC has a relatively smooth geometrical shape.

Extending the study of star pairs to larger angular separations, we find that the values of $N_{\text{H I}}(\text{LIC})$ usually

agree to better than a factor of 2.0 (and often to within a factor of 1.5) for separations up to 43° , but the disagreements are mostly greater than a factor of 2.0 for larger separations. We conclude that the surface of the LIC is relatively smooth on scales up to 43° , if our assumption of constant density is approximately valid. The only exception to this conclusion is the region near $l = 220^\circ$ and the Galactic plane which includes Sirius, Procyon, and the ϵ CMA interstellar tunnel. This gives us confidence that it may be possible to fit the LIC with a relatively smooth geometric surface.

There are 26 star pairs in Table 4 for which we have GHRS and/or *EUVE* spectroscopic measurements of $N_{\text{H I}}(\text{total})$, which includes the amount of warm gas in the LIC and other clouds. Now the comparison is more mixed as nine pairs are category A, four are category B, two are category C, and 11 are category D. However, if we consider only the nine star pairs in which both stars lie within 60 pc, then four are in category A, three in category B, two in category C, and none in category D. Thus, within 60 pc of the Sun, the total amount of warm gas does not vary greatly on angular scales less than 20° .

4.2. How Close Is the G Cloud?

Lallement & Bertin (1992) have put forward two convincing arguments that the LIC velocity vector is representative of the ISM surrounding the heliosphere: (a) inside the heliosphere the velocity of neutral helium, which should not be deflected or decelerated by interactions with the solar wind, is consistent with the LIC velocity; and (b) lines of sight in nearly all directions show interstellar absorption features within 1 km s^{-1} of the projected LIC velocity. The two clear exceptions are the lines of sight to α Cen, which shows absorption *only* at the projected velocity of the G cloud (Linsky & Wood 1996), and toward the north Galactic pole star 31 Com (Piskunov et al. 1997) and HZ 43 (Landsman, Sofia, & Bergeron 1996). Since the projected velocities for the LIC and G cloud differ by 2.4 km s^{-1} toward α Cen A and B, the GHRS echelle spectra of the Mg II lines toward these stars should show absorption components at both projected velocities, unless the Sun lies extremely close to the boundary between the two clouds, as Figure 1 suggests.

How close to the Sun is the boundary between the LIC and the G cloud? Lallement et al. (1995) estimate that the upper limit to the Mg II column density at the LIC velocity is only 2%–4% of the total Mg II column density. If the upper limit on the fraction of neutral hydrogen at the LIC velocity is the same as for Mg II, we estimate that the boundary of the two clouds is at $\leq 0.054 \text{ pc}$ from the Sun in the direction of α Cen. Since the LIC flow velocity in this direction is -18.0 km s^{-1} , the boundary should reach the heliosphere in $\leq 3000 \text{ yr}$, a very short time interval by astronomical standards. The densities of neutral hydrogen in the two clouds are about the same, but the density in the boundary layer at the cloud interface could be much larger as the G cloud is overtaking the LIC. It would be interesting to estimate the density of the boundary layer and its thickness, which should depend on the magnetic field properties. One could then estimate the changes in the heliosphere shape and properties when the boundary layer will eventually interact with the heliosphere. The study of the LIC-G cloud interaction by Grzedzielski & Lallement

TABLE 4
COMPARISON OF INTERSTELLAR PARAMETERS FOR STAR PAIRS

SEPARATION (deg) (1)	STAR PAIRS (2)	DATA SOURCE (3)	DISTANCE (pc) (4)	$N_{\text{H I}}$ (10^{17} cm^{-2})		AGREEMENT	
				Total (5)	LIC (6)	Total (7)	LIC (8)
0.9	β Gem	GHR	10.3	18	13	A	A
	σ Gem	GHR	37.5	15	11		
2.0	ϵ Ind	GHR	3.63	11	?	D	...
	REJ 2156–546	<i>EUVE</i>	129	59	...		
3.4	HR 1099	GHR	29.0	14	8.3	B	...
	GD 50	<i>EUVE</i>	37	8.7	...		
5.1	Sirius A	GHR	2.63	3.6	1.8	D	...
	Sirius B	<i>EUVE</i>	2.63	5.2	?	D	...
	β CMa	<i>EUVE</i>	153	20:	...		
		GHR	153	>17	...		
5.6	HZ 43	<i>EUVE</i>	32.0	8.7	...	A	...
		GHR	32.0	8.7	≤ 0.9		
	31 Com	GHR	94.2	8.7	≤ 0.3		
5.8	ϵ CMa	GHR	132	4:	...	D	...
	REJ 0720–318	<i>EUVE</i>	136	23	...		
6.9	GD 153	<i>EUVE</i>	69	8.8	...	A	...
	31 Com	GHR	94.2	8.7	≤ 0.3		
7.2	Capella	GHR	12.9	19	19	A	A
	G191-B2B	<i>EUVE</i>	68.8	21	...		
		STIS	68.8	20	17		
9.0	HZ 43	<i>EUVE</i>	32.0	8.7	...	A	...
		GHR	32.0	8.7	≤ 0.9		
	GD 153	<i>EUVE</i>	69	8.8	...		
9.8	ϵ Eri	GHR	3.22	7.1	7.1	C	A
	HR 1099	GHR	29.0	14	8.3		
10.6	ϵ Eri	GHR	3.22	7.1	7.1	A	A
	40 Eri A	GHR	5.04	7.1	7.1		
11.0	40 Eri A	GHR	5.04	7.1	7.1	A	...
	GD 50	<i>EUVE</i>	37	8.7	...		
11.1	ϵ Eri	GHR	3.22	7.1	7.1	A	...
	GD 50	<i>EUVE</i>	37	8.7	...		
11.4	ϵ Ind	GHR	3.63	11	...	D	...
	REJ 2324–547	<i>EUVE</i>	185	40	...		
12.3	REJ 2156–546	<i>EUVE</i>	129	59	...	B	...
	REJ 2324–547	<i>EUVE</i>	185	40	...		
12.9	40 Eri A	GHR	5.04	7.1	7.1	B	A
	HR 1099	GHR	29.0	14	8.3		
13.0	Sirius	GHR	2.63	3.6	1.8	A	C
	ϵ CMa	<i>EUVE</i>	132	9:	...		
		GHR	132	4:	2.8:		
14.0	ϵ CMa	<i>EUVE</i>	132	10:	...	D	...
		GHR	132	4:	2.8:		
	β CMa	<i>EUVE</i>	153	20:	...		
		GHR	153	>17	...		
14.4	β Cas	GHR	16.7	15	15	C	...
	λ And	GHR	25.8	32	?		
15.0	β Cet	GHR	29.4	34	?	B	...
	GD 659	<i>EUVE</i>	58	26	...		
15.0	ϵ Ind	GHR	3.63	11	...	D	...
	REJ 2009–605	<i>EUVE</i>	62	210	...		
15.1	REJ 2009–605	<i>EUVE</i>	62	210	...	D	...
	REJ 2156–546	<i>EUVE</i>	129	59	...		
15.4	HR 1099	GHR	29.0	14	8.3	D	...
	Feige 24	<i>EUVE</i>	74.4	30	...		
17.9	Sirius	GHR	2.63	3.6	1.8	D	...
	REJ 0720–318	<i>EUVE</i>	136	23	...		
18.5	GD 50	<i>EUVE</i>	37	8.7	...	D	...
	Feige 24	<i>EUVE</i>	90	30	...		
19.7	ϵ Eri	GHR	3.22	7.1	7.1	D	...
	Feige 24	<i>EUVE</i>	74.4	30	...		

(1996) concludes that the two clouds are in contact with an MHD shock front propagating from the LIC into the G cloud. The existence of a nearby incoming cloud has been proposed (Vidal-Madjar et al. 1978), and there are predictions of significant changes in the terrestrial climate if the cloud has densities exceeding 10^3 hydrogen atoms cm^{-3} (Begelman & Rees 1976) or 10^6 hydrogen atoms cm^{-3} (McCrea 1975).

5. CONCLUSIONS

In this first paper in a series on the structure of the LISM, we develop a methodology for estimating the distance to the outer edge of the LIC based on interstellar hydrogen column densities derived from high-resolution GHRS spectra and *EUVE* spectra of nearby stars. In subsequent papers we will apply this methodology to construct and visualize three-dimensional models for the LIC and other nearby warm clouds in the LISM based on GHRS, *EUVE*, and ground-based spectra. Our methodology and the conclusions of Paper I are summarized below:

1. Our working definition of a warm interstellar cloud is a volume of space with roughly constant density, ionization, temperature, and gas phase abundances (or depletions onto grains) that moves with a common bulk velocity vector. Although the shape of the cloud could be very irregular, presumably controlled by external gas and magnetic pressures and radiation fields, the roughly constant physical and chemical properties imply a well-mixed gas with a common history. Although this concept of a cloud is perhaps too idealized, the properties of the LIC sampled along many lines of sight are sufficiently similar to make this concept credible. The construction of models for the LIC and other nearby clouds is important for estimating hydrogen column densities along unobserved lines of sight and for studying the response of the clouds to external pressures and radiation fields.

2. Published interstellar column densities are now available from high- or medium-resolution GHRS spectra of the H I and D I Ly α lines for 21 lines of sight toward stars located within about 153 pc. In most cases there are also spectra of metal lines (e.g., Fe II and Mg II) from which one can infer the velocity structure along these lines of sight and thereby estimate the fraction of the H I column density at the projected LIC velocity. Given the saturation of the H I Ly α line and the presence of hydrogen walls around the Sun and many target stars that complicate direct measurements of H I absorption, we believe that the most accurate H I column densities are derived from the measured D I column densities and the mean D/H ratio in the LIC. Using this method we derive H I column densities (or upper limits) through the LIC for 16 lines of sight toward 12 cool stars or binary systems, two hot stars, and two hot white dwarfs.

3. A number of stars have velocities and/or depletions that indicate absorption by other warm clouds in their lines of sight. For example, α Cen A and B show interstellar absorption velocity at a single velocity that indicates that these stars lie in the G cloud. ϵ Ind probably also lies in this cloud. Both HZ 43 and 31 Com show interstellar absorption at a velocity inconsistent with the LIC and G vectors and thus lie in another cloud, which we call the north Galactic pole cloud. β Cet shows an absorption component consistent with the LIC vector but with very different magnesium and iron depletions than typically seen in the LIC.

We therefore assign this absorption to another cloud which we call the south Galactic pole cloud.

4. Published interstellar H I column densities obtained from the analysis of *EUVE* spectra are now available for 39 lines of sight toward hot white dwarfs, B-type stars, and cataclysmic binaries located within 200 pc of the Sun. These H I column densities refer to the total H I column density along the line of sight, which cannot be assigned to individual clouds without additional information. Hydrogen column densities for the lines of sight toward four white dwarfs (Sirius B, HZ 43, G191-B2B, and REJ 1032+535) have now been measured using GHRS, STIS, and *EUVE* data. For the Sirius line of sight the comparison is between GHRS spectra of the A-type star Sirius A and *EUVE* spectra of the white dwarf Sirius B. Since the total H I column densities derived by these two independent and very different techniques are in excellent agreement for HZ 43, G191-B2B, and REJ 1032+535 and differ by only 30% for Sirius A compared to Sirius B, we believe that the hydrogen column densities derived from *EUVE* spectra can also be used in constructing cloud models. The accuracy of the *EUVE* hydrogen column densities is likely lower than the GHRS derived values as theoretical extreme ultraviolet spectra of white dwarfs may not contain all of the important opacity sources. Comparison of hydrogen column densities derived from *EUVE* spectra and WFC photometry show very large discrepancies, so the photometric column densities do not provide useful constraints on the cloud morphologies.

5. Comparison of LIC and total hydrogen column densities toward pairs of stars with separations between 0.9° and 20° reveals a pattern of good agreement so long as both stars lie within 60 pc of the Sun. Thus the LIC and perhaps also other nearby warm clouds have shapes that do not change rapidly on these angular scales. The only exception identified so far is the region near $l = 220^\circ$ close to the Galactic plane including Sirius, Procyon, G191-B2B, and the ϵ CMa interstellar tunnel where the photoionizing radiation from ϵ CMa appears to carve out sharp structure in the LISM. In Paper II we will therefore fit the shape of the LIC with a set of smooth basis functions (spherical harmonics).

6. We compute distances to the edge of the LIC along each line of sight by assuming that all interstellar gas moving with a speed consistent with the LIC velocity vector has a constant density, $n_{\text{H I}} = 0.10 \text{ cm}^{-3}$, and the LIC extends from the heliosphere to an edge determined by the value of $N_{\text{H I}}$ moving at this speed. The computed distances to the edge of the LIC show that the Sun is located inside the LIC but very close to its edge toward the Galactic center and the NGP. The absence of Mg II absorption at the LIC velocity toward α Cen indicates that the distance to the edge of the LIC in this direction is ≤ 0.05 pc. The Sun should leave the LIC and probably enter the G cloud in less than 3000 yr.

This work is supported by NASA grant S-56460-D to the National Institute of Standards and Technology. We thank Dr. M. Sahu for permitting us to include her results for the G191-B2B line of sight before publication.

REFERENCES

- Barstow, M. A., Dobbie, D. P., Holberg, J. B., Hubeny, I., & Lanz, T. 1997, *MNRAS*, 286, 58
- Barstow, M. A., Holberg, J. B., Hubeny, I., Lanz, T., Bruhweiler, F. C., & Tweedy, R. W. 1996, *MNRAS*, 279, 1120
- Barstow, M. A., Holberg, J. B., & Koester, D. 1995a, *MNRAS*, 274, L31
- Barstow, M. A., Jordan, S., O'Donoghue, D., Burleigh, M. R., Napiwotzki, R., & Harrop-Allin, M. K. 1995b, *MNRAS*, 277, 971
- Begelman M. C., & Rees, M. J. 1976, *Nature*, 261, 298
- Bertin, P., Vidal-Madjar, A., Lallement, R., Ferlet, R., & Lemoine, M. 1995, *A&A*, 302, 889
- Bruhweiler, F. C. 1996, in *Astrophysics in the Extreme Ultraviolet*, ed. S. Bowyer & R. F. Malina (Dordrecht: Kluwer), 261
- Burleigh, M. R., Barstow, M. A., & Dobbie, P. D. 1997, *A&A*, 317, L27
- Cassinelli, J. P., et al. 1995, *ApJ*, 438, 932
- . 1996, *ApJ*, 460, 949
- Clarke, J. T., Lallement, R., Bertaux, J.-L., Fahr, H., Quémerais, E., & Scherer, H. 1998, *ApJ*, 499, 482
- Cox, D. P. & Reynolds, R. J. 1987, *ARA&A*, 25, 303
- Craig, N. et al. 1997, *ApJS*, 113, 131
- Crutcher, R. M. 1982, *ApJ*, 254, 82
- Cully, S. L., et al. 1996, in *Astrophysics in the Extreme Ultraviolet*, ed. S. Bowyer & R. F. Malina (Dordrecht: Kluwer), 349
- Dring, A., Linsky, J., Murthy, J., Henry, R. C., Moos, H., Vidal-Madjar, A., Audouze, J., & Landsman, W. 1997, *ApJ*, 488, 760
- Dupin O., & Gry, C. 1998, *A&A*, 335, 661
- Dupuis, J., & Vennes, S. 1996, in *Astrophysics in the Extreme Ultraviolet*, ed. S. Bowyer & R. F. Malina (Dordrecht: Kluwer), 217
- . 1997, *ApJ*, 475, L131
- Dupuis, J., Vennes, S., Bowyer, S., Pradhan, A. K., & Thejll, P. 1995, *ApJ*, 455, 574
- Ferlet, R., Lallement, R., & Vidal-Madjar, A. 1986, *A&A*, 163, 204
- Ferlet, R., Lemoine, M., & Vidal-Madjar, A. 1996, in *Science with the Hubble Space Telescope—II*, ed. P. Benvenuti, F. D. Macchetto, & E. J. Schreier (Baltimore: STScI), 449
- Frisch, P. C. 1990, in *COSPAR Colloq. Ser. 1, Physics of the Outer Heliosphere*, ed. S. Grzedziński & E. Page (New York: Pergamon), 19
- . 1994, *Science*, 265, 1423
- . 1995, *Space Sci. Rev.*, 72, 499
- . 1996, *Space Sci. Rev.*, 78, 213
- Frisch, P. C., & York, D. G. 1983, *ApJ*, 271, L59
- Gayley, K. G., Zank, G. P., Pauls, H. L., Frisch, P. C., & Welty, D. E. 1997, *ApJ*, 487, 259
- Génova, R., Malaro, P., Vladilo, G., & Beckman, J. E. 1990, *ApJ*, 355, 150
- Gry, C., Lemonon, L., Vidal-Madjar, A., Lemoine, M., & Ferlet, F. 1995, *A&A*, 302, 497
- Gry, C., York, D. G., & Vidal-Madjar, A. 1985, *ApJ*, 296, 593
- Grzedziński, S., & Lallement, R. 1996, *Space Sci. Rev.*, 78, 247
- Holberg, J. B., Barstow, M. A., Bruhweiler, F. C., Cruise, A. M., & Penny, A. J. 1998a, *ApJ*, 497, 935
- Holberg, J. B., Barstow, M. A., Bruhweiler, F. C., & Sion, E. M. 1995, *ApJ*, 453, 313
- Holberg, J. B., Barstow, M. A., & Sion, E. M. 1998b, *ApJS*, 119, 207
- Holberg, J. B., Bruhweiler, F. C., Barstow, M. A., & Dobbie, P. D. 1999, *ApJ*, 517, 841
- Jenkins, E. B., Tripp, T. M., Wozniak, P. R., Sofia, U. J., & Sonneborn, G. 1999, poster presented at 193d AAS Meeting, Austin, TX, 1999 January
- Lallement, R., & Bertin, P. 1992, *A&A*, 266, 479
- Lallement, R., Ferlet, R., Lagrange, A. M., Lemoine, M., & Vidal-Madjar, A. 1995, *A&A*, 304, 461
- Landsman, W., Sofia, U. J., & Bergeron, P. 1996, in *Science with the Hubble Space Telescope—II*, ed. P. Benvenuti, F. D. Macchetto, & E. J. Schreier (Baltimore: STScI), 454
- Lanz, T., Barstow, M. A., Hubeny, I., & Holberg, J. B. 1996, *ApJ*, 473, 1089
- Lemoine, M., Vidal-Madjar, A., Bertin, P., Ferlet, R., Gry, C., & Lallement, R. 1996, *A&A*, 308, 601
- Long, K. S., Mauche, C. W., Raymond, J. C., Szkody, P., & Mattei, J. A. 1996, *ApJ*, 469, 841
- Linsky, J. L. 1998, *Space Sci. Rev.*, 84, 285
- Linsky, J. L., et al. 1993, *ApJ*, 402, 694
- Linsky, J. L., Diplas, A., Wood, B. E., Brown, A., Ayres, T. R., & Savage, B. D. 1995, *ApJ*, 451, 335
- Linsky, J. L., & Redfield, S. 1999, *BAAS*, 31, 890
- Linsky, J. L., & Wood, B. E. 1996, *ApJ*, 463, 254
- Lyu, C.-H., & Bruhweiler, F. C. 1996, *ApJ*, 459, 216
- Marsh, M. C., et al. 1997, *MNRAS*, 287, 705
- Mauche, C. W., Raymond, J. C., & Mattei, J. A. 1995, *ApJ*, 446, 842
- McClintock, W., Henry, R. C., Linsky, J. L., & Moos, H. W. 1978, *ApJ*, 225, 465
- McCrea, W. H. 1975, *Nature*, 255, 607
- Meyer, D. M., & Blades, J. C. 1996, *ApJ*, 464, L179
- Mullan, D. J., & Linsky, J. L. 1999, *ApJ*, 511, 502
- Munch, G., & Unsold, A. 1962, *ApJ*, 135, 711
- Napiwotzki, R., et al. 1996, in *Astrophysics in the Extreme Ultraviolet*, ed. S. Bowyer & R. F. Malina (Dordrecht: Kluwer), 241
- Paerels, F., Hur, M. Y., Mauche, C. W., & Heise, J. 1996, *ApJ*, 464, 884
- Paresce, F. 1984, *AJ*, 89, 1022
- Perryman, A. C., & the Hipparcos Science Team. 1997, in *The Hipparcos and Tycho Catalogues* (ESA SP 1200; Noordwijk: ESA)
- Piskunov, N., Wood, B. E., Linsky, J. L., Dempsey, R. C., & Ayres, T. R. 1997, *ApJ*, 474, 315
- Quémerais, E., Sandel, B. R., Lallement, R., & Bertaux, J.-L. 1995, *A&A*, 299, 249
- Redfield, S., & Linsky, J. L. 2000, *ApJ*, in press
- Sahu, M. S., et al. 1999, *ApJ*, 523, L159
- Savage, B. D., & Sembach, K. R. 1996, *ARA&A*, 34, 279
- Scherer, H., Bzowski, M., Fahr, H. J., Ruci, N., & Ski, D. 1999, *A&A*, 342, 601
- Sembach, K. R., & Savage, B. D. 1996, *ApJ*, 457, 211
- Szkody, P., Vennes, S., Sion, E. M., Long, K. S., & Howell, S. B. 1997, *ApJ*, 487, 916
- Vallerga, J. V., Vedder, P. W., Craig, N., & Welsh, B. Y. 1993, *ApJ*, 411, 729
- Vallerga, J. V., & Welsh, B. Y. 1995, *ApJ*, 444, 702
- Vennes, S., Bowyer, S., & Dupuis, J. 1996a, *ApJ*, 461, L103
- Vennes, S., Christian, D. J., & Thorstensen, J. R. 1998, *ApJ*, 502, 763
- Vennes, S., Dupuis, J., Bowyer, S., & Pradhan, A. K. 1997b, *ApJ*, 482, L73
- Vennes, S., Dupuis, J., Rumph, T., Drake, J., Bowyer, S., Chayer, P., & Fontaine, G. 1993, *ApJ*, 410, L119
- Vennes, S., Szkody, P., Sion, E. M., & Long, K. S. 1995, *ApJ*, 445, 921
- Vennes, S., Thejll, P. A., Wickramasinghe, D. T., & Bessel, M. S. 1996b, *ApJ*, 467, 782
- Vidal-Madjar, A., Laurent, C., Burston, P., & Audouze, J. 1978, *ApJ*, 223, 589
- Vidal-Madjar, A., et al. 1998, *A&A*, 338, 694
- Walker, T. P., Steigman, G., Schramm, D. N., Olive, K. A., & Kang, H. S. 1991, *ApJ*, 376, 51
- Welsh, B. Y. 1991, *ApJ*, 373, 556
- Welty, D. E., Morton, D. C., & Hobbs, L. M. 1996, *ApJS*, 106, 533
- Witte, M., Rosenbauer, H., Banaszekiewicz, M., & Fahr, H. 1993, *Adv. Space Res.*, 13, 121
- Wood, B. E., Alexander, W. R., & Linsky, J. L. 1996, *ApJ*, 470, 1157
- Wood, B. E., & Linsky, J. L. 1997, *ApJ*, 474, L39
- . 1998, *ApJ*, 492, 788
- York, D. G., & Frisch, P. C. 1984, in *Local Interstellar Medium* (NASA CP-2345; Greenbelt: NASA), 51
- York, D. G., & Rogerson, J. B. 1976, *ApJ*, 203, 378